High-spin states in ^{96,97}Nb

N. Fotiades*
Los Alamos National Laboratory, Los Alamos, New Mexico 87545, USA

J. A. Cizewski
Department of Physics and Astronomy, Rutgers University, New Brunswick, New Jersey 08903, USA

R. Krücken
Physik Department E12, Technische Universität München, D-85748 Garching, Germany

R. M. Clark, P. Fallon, I. Y. Lee, and A. O. Macchiavelli
Nuclear Science Division, Lawrence Berkeley National Laboratory, Berkeley, California 94720, USA

J. A. Becker and W. Younes
Lawrence Livermore National Laboratory, Livermore, California 94550, USA
(Received 6 August 2010; revised manuscript received 20 September 2010; published 7 October 2010)

The high-spin level structures of the ^{96,97}Nb isotopes have been studied. The isotopes were produced in the fission of the compound systems formed in two heavy-ion-induced reactions, ^{24}Mg (134.5 MeV) + ^{173}Yb and ^{23}Na (129 MeV) + ^{176}Yb. Gamma-ray spectroscopy was accomplished with the Gammasphere array. High-spin states are observed for the first time in both isotopes with excitation energies up to 5.2 and 6.6 MeV in ^{96,97}Nb, respectively. The coupling of the odd proton occupying the $g_{9/2}$ orbital to the yrast states in the subshell closure nucleus of ^{96}Zr can account for the first excited states of ^{97}Nb. A comparison with the first excited states in ^{95}Zr is also attempted. The addition of a neutron hole in ^{96}Nb results in a much more fragmented level scheme.

DOI: 10.1103/PhysRevC.82.044306 PACS number(s): 23.20.Lv, 27.60.+j

I. INTRODUCTION

The spectroscopic study of high-spin states of ^{96,97}Nb is very interesting because these isotopes differ by one or two particles from the subshell closure nucleus of $^{96}Zr_{56}$. There is a plethora of spectroscopic information in the immediate vicinity of the subshell closure nucleus of $^{90}Zr_{50}$. In contrast, high-spin-state information for nuclei neighboring ^{96}Zr is much more limited. This is due, in part, to their proximity to the line of stability which makes difficult the population of these isotopes as evaporation residues in heavy-ion fusion reactions with stable beam-target combinations. Hence, the study of high-spin states in ^{96,97}Nb brings new information important for understanding the coupling of nucleons to the subshell closure that occurs in ^{96}Zr.

The ^{97}Nb isotope has only one proton more than ^{96}Zr. The limited spectroscopic information that exists for this nucleus is summarized in Ref. [1] and comes from particle pick-up reactions and the β decay of ^{97}Zr. Only low-spin states (spin lower than the $9/2^+$ ground state) are known. The spin and parity of the ground state originate from the odd proton occupying the $g_{9/2}$ orbital. Theoretical attempts to predict states in this nucleus have been limited to low-spin negative-parity states [2,3], except for the shell-model calculations in Refs. [4,5] where the first $13/2^+$ state is predicted at $\sim$1.5 MeV and $\sim$0.6 MeV excitation energy, respectively.

The odd-odd ^{96}Nb isotope has one proton more and one neutron less than ^{96}Zr. The limited spectroscopic information that exists for this nucleus is summarized in Ref. [6] and comes from particle pick-up reactions. Several low-spin excited states above the 6^+ ground state and one higher-spin state, (7^+) at 233(5)-keV excitation energy, have been observed. No transition was reported to deexcite the latter. Previous theoretical attempts to predict states in this nucleus were limited to low-spin states [7], except for the shell-model calculation in Ref. [4] where the first 7^+ state is predicted at $\sim$0.5 MeV excitation energy.

For nuclei near ^{96}Zr (e.g., ^{94,95,96}Y, ^{95,97}Zr, and ^{96,97,98}Nb) high-spin states are known in ^{95,96}Zr [8,9] and in ^{95}Y [10] from γ-ray spectroscopy of fission fragments, which is an alternative way to study these nuclei near the line of stability (see, for instance, Refs. [11,12] and references therein). Such technique was used extensively in the past to study high-spin states in nuclei near the line of stability, is complementary to studies based on Coulomb excitation and deep-inelastic processes, and helps bridge the gap in high-spin-state systematics in areas between the neutron-deficient and neutron-rich nuclei [11]. In the present work we used this technique to identify high-spin states in ^{96,97}Nb.

II. EXPERIMENTS

The 88-Inch Cyclotron Facility at Lawrence Berkeley National Laboratory and the Gammasphere array were used to populate compound nuclei and for subsequent γ-ray

*fotia@lanl.gov

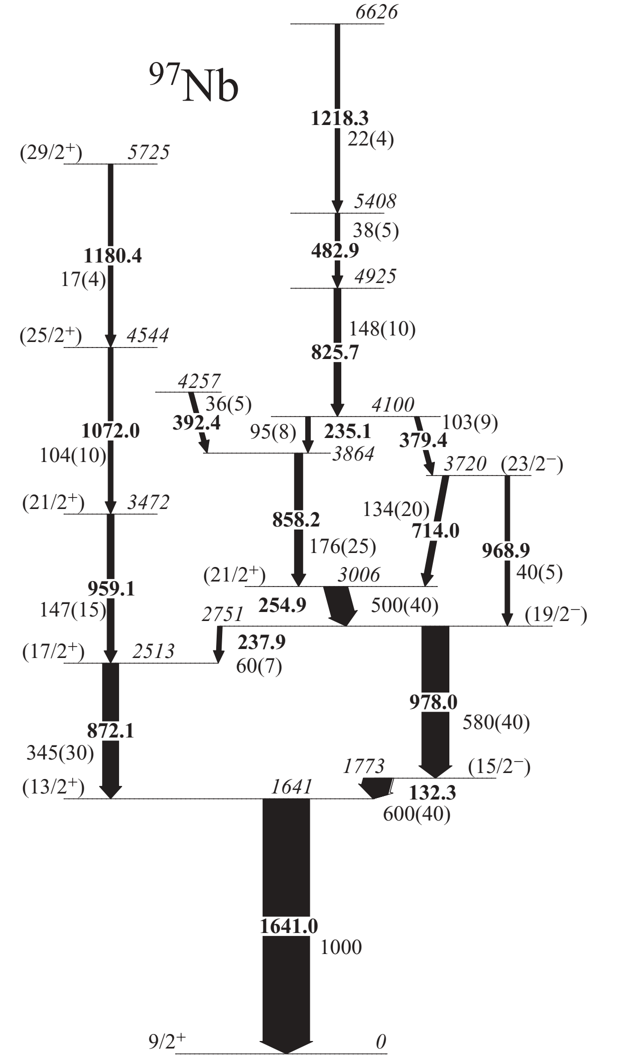

FIG. 1. Level scheme assigned to ^{97}Nb in the present work. Transition and excitation energies are given in keV. The widths of the arrows are representative of the relative intensity of the transitions, which is quoted for each transition. The uncertainty on the γ-ray energies varies from 0.4 to 0.9 keV.

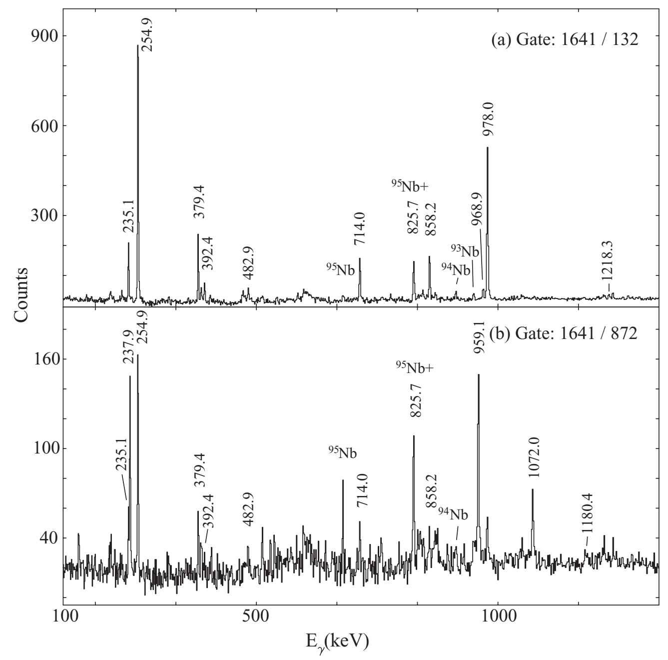

FIG. 2. Background subtracted spectra from the ^{197}Pb(CN) experiment gated on pairs of transitions (1641.0-, 132.3-keV and 1641.0-, 872.1-keV pairs) assigned to ^{97}Nb in the present work. The energies of the transitions are in keV. Transitions associated with the complementary ^{93}Nb [15], ^{94}Nb [16], and ^{95}Nb [17] isotopes are indicated. Unlabeled peaks in both spectra are most likely contaminants.

spectroscopy in two similar experiments henceforth referred to as Experiments I and II. In Experiment I, Gammasphere comprised 92 Compton-suppressed large-volume HPGe detectors, whereas in Experiment II the number of Ge detectors was 100. The “heavimet” collimators for the escape suppression shields of Gammasphere were mounted during both experiments, hence, no information was possible to be extracted from “H-K” gating using the total γ-ray energy absorbed and the γ-ray multiplicity.

In Experiment I, a ^{197}Pb compound nucleus (CN) was formed in the ^{24}Mg + ^{173}Yb reaction at 134.5 MeV. The target consisted of 1 mg/cm^2 isotopically enriched ^{173}Yb, evaporated on a 7 mg/cm^2 gold backing (reactions of the beam in the backing produce a ^{221}Pa CN). In Experiment II a ^{199}Tl CN was formed in the ^{23}Na + ^{176}Yb reaction at a beam energy of 129 MeV. The target consisted of approximately 1 mg/cm^2 isotopically enriched ^{176}Yb on a 10 mg/cm^2 Au backing (reactions of the beam in the backing produce a ^{220}Th CN).

About 2.3×10^9 triples and 10^9 quadruples were collected in Experiment I and II, respectively. Symmetrized, three-dimensional cubes were constructed in all cases to investigate the coincidence relationships between the γ rays. Additional information for both experiments in the present work can be found in Refs. [13,14].

III. EXPERIMENTAL RESULTS

A. Levels and transitions in ^{97}Nb

The level scheme of ^{97}Nb deduced in the present work is shown in Fig. 1; intensities of the transitions obtained in Experiment I are quoted. This is the first observation of high-spin states in this nucleus, whereas previous information [1] on the structure of ^{97}Nb was obtained from particle transfer reactions and the β decay of ^{97}Zr. Eighteen new transitions and 15 new states are included in the level scheme establishing excitations up to ~6.6-MeV excitation energy.

The quality of the data obtained in Experiment I can be seen in the gated spectra in Fig. 2. Most of the transitions assigned to ^{97}Nb are present in the spectra in Fig. 2. Transitions from the complementary fragments ^{93}Nb [15], ^{94}Nb [16], and ^{95}Nb [17] relative to the ^{197}Pb compound nucleus are also indicated. Above the energies shown, there were no statistically significant peaks in the spectra in Fig. 2.

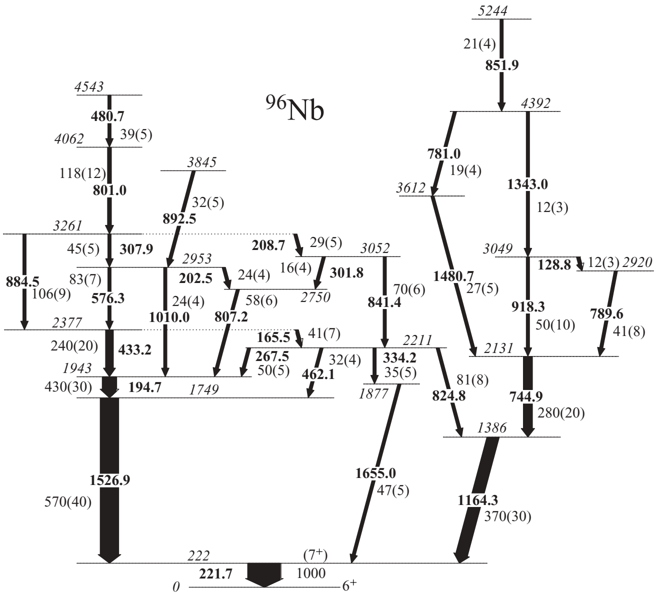

FIG. 3. Level scheme assigned to ^{96}Nb in the present work. Transition and excitation energies are given in keV. The widths of the arrows are representative of the relative intensity of the transitions, which is quoted for each transition. The uncertainty on the γ-ray energies varies from 0.4 to 0.9 keV.

Spin and parity assignments of all levels of ^{97}Nb reported in this work are difficult to deduce experimentally because of the lack of directional correlation information for the fission products. However, based on comparison with experimental results on the first excited states in ^{96}Zr [9], spin and parity assignments for many levels in Fig. 1 are tentatively suggested (see discussion below).

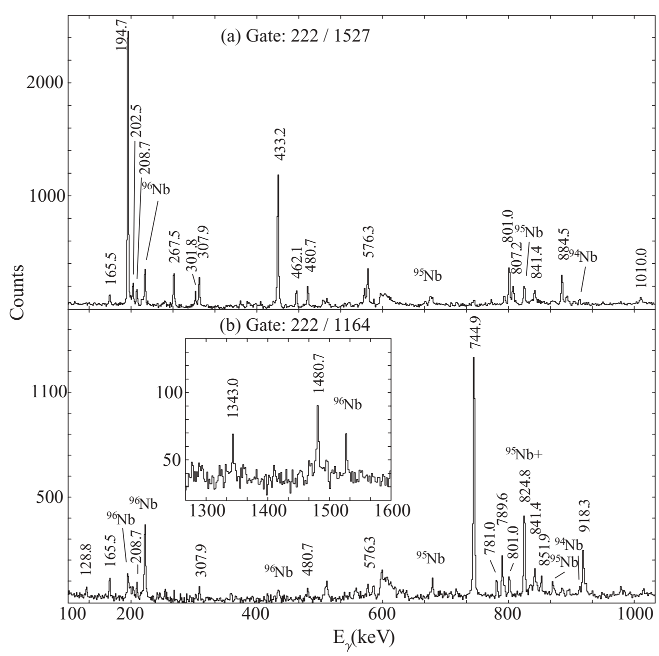

FIG. 4. Background subtracted spectra from the ^{197}Pb(CN) experiment gated on pairs of transitions (221.7-, 1526.9-keV and 221.7-, 1164.3-keV pairs) assigned to ^{96}Nb in the present work. The energies of the transitions are in keV. Transitions associated with the complementary ^{94}Nb [16] and ^{95}Nb [17] isotopes are indicated. ^{96}Nb is also a complementary fragment to itself. Unlabeled peaks in both spectra are most likely contaminants.

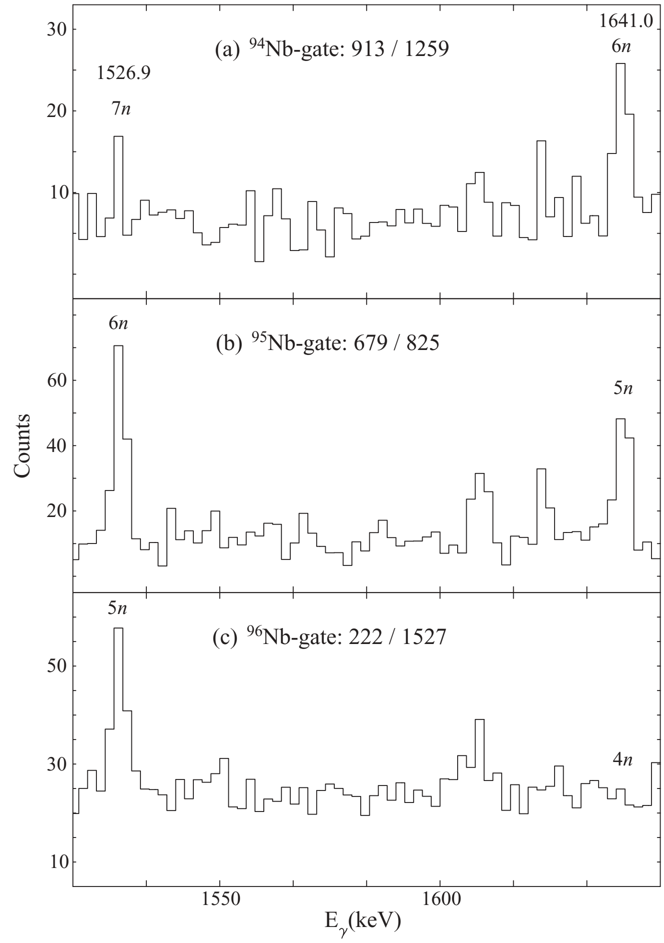

FIG. 5. Background subtracted spectra from the ^{197}Pb(CN) experiment gated on transitions belonging to (a) ^{94}Nb [16], 912.6- and 1258.85-keV transitions, (b) ^{95}Nb [17], 679.0- and 824.7-keV transitions, and (c) ^{96}Nb, 221.7- and 1526.9-keV transitions. The energies of the transitions are in keV. The 1526.9- and 1641.0-keV transitions assigned to ^{96,97}Nb isotopes, respectively, in the present work are indicated. ^{96}Nb is a complementary fragment to itself, hence the presence of the 1526.9-keV transition in the lower spectrum. Unlabeled peaks are most likely contaminants.

B. Levels and transitions in ^{96}Nb

The existing information [6] on the structure of ^{96}Nb was obtained only from particle transfer reactions. The level scheme of ^{96}Nb deduced in the present work is shown in Fig. 3 and the intensities of the transitions obtained in Experiment I are quoted. This is the first observation of high-spin states in this nucleus. Thirty-one new transitions and 19 new states are included in the level scheme establishing excitations up to ∼5.2-MeV excitation energy. Thus, the level scheme for this nucleus is substantially enriched with more than doubling the number of transitions known in this nucleus.

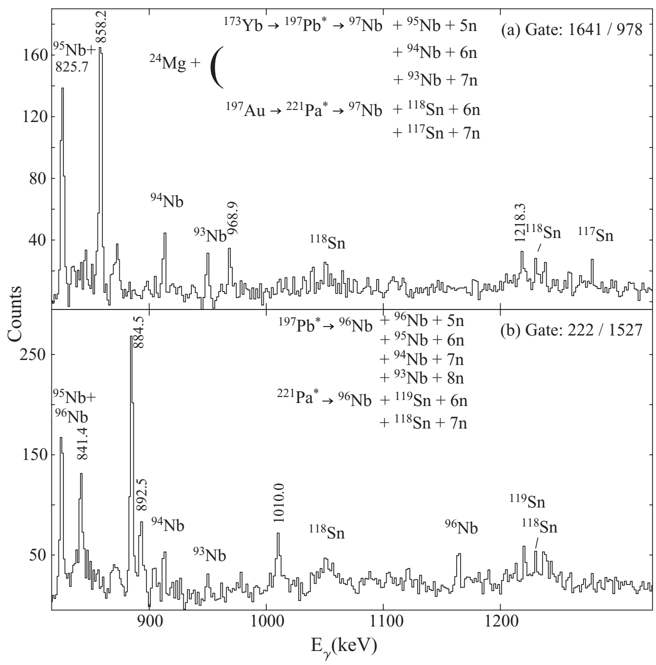

FIG. 6. Background subtracted spectra from the ^{197}Pb(CN) experiment gated on transitions assigned to (a) ^{97}Nb (1641.0- and 978.0-keV) and (b) ^{96}Nb (221.7- and 1526.9-keV) in the present work. The energies of the transitions are in keV. Transitions associated with the complementary ^{93}Nb [15], ^{94}Nb [16], and ^{95}Nb [17] isotopes, with respect to reactions in the target, and the complementary ^{117}Sn [20], ^{118}Sn [21], and ^{119}Sn [22], with respect to reactions in the backing, are indicated. ^{96}Nb is also a complementary fragment to itself. Unlabeled peaks in both spectra are most likely contaminants.

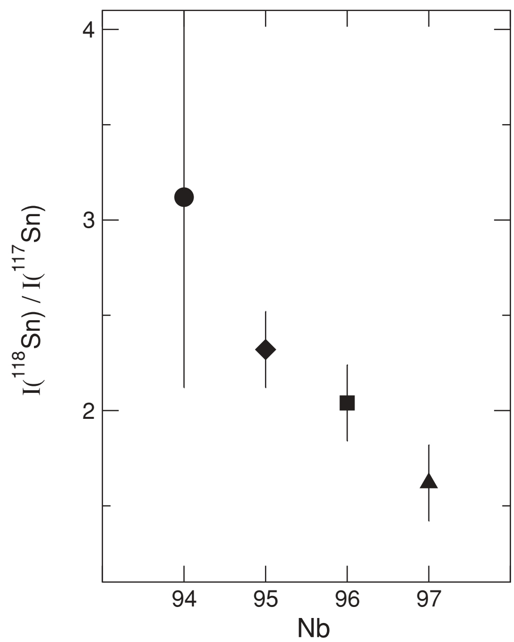

FIG. 7. Ratios of intensities of transitions in Nb isotopes observed in spectra gated on ^{117}Sn [20] and ^{118}Sn [21] in the ^{197}Pb(CN) experiment. The known transitions in ^{94}Nb [16] (912.6 keV, circle), and ^{95}Nb [17] (824.7 keV, diamond), were used, as well as the 194.7-keV (square) and 1641.0-keV (triangle) transitions assigned to ^{96,97}Nb, respectively, in the present work. The intensity values are given in Table I.

Several transitions from Fig. 3 can be seen in the gated spectra in Fig. 4 obtained in Experiment I. Transitions from the complementary fragments ^{94}Nb [16] and ^{95}Nb [17] relative to the ^{197}Pb compound nucleus are also indicated. Above the energies shown, there were no statistically significant peaks in the spectra in Fig. 4. ^{96}Nb is a complementary fragment to itself in the ^{197}Pb (CN) experiment (i.e., $^{197}\text{Pb}^* \rightarrow {}^{96}\text{Nb} + {}^{96}\text{Nb} + 5n$) and the transitions labeled as "^{96}Nb" in Fig.4 are present in the spectra for this reason. The same phenomenon was observed for the ^{95}Nb fragments in the ^{197}Pb (CN) experiment (i.e., $^{197}\text{Pb}^* \rightarrow {}^{95}\text{Nb} + {}^{95}\text{Nb} + 7n$).

As in ^{97}Nb, spin and parity assignments of all levels of ^{96}Nb reported in this work are difficult to deduce experimentally. The only exception is the first excited state in Fig. 3, which is most likely the previously known (7^+) state at 233(5)-keV excitation energy [6], hence, the proposed spin-parity assignment in Fig. 3.

C. Assignment of transitions

The assignment of the transitions in Figs. 1 and 3 to ^{97}Nb and ^{96}Nb, respectively, was based on the coincidences established between these transitions and transitions from complementary fragments in both experiments. Both isotopes are populated stronger as fragments in the ^{197}Pb(CN) experiment where the Nb isotopes are predicted by a statistical model to be at the peak of the fission fragment Z distribution [18]. Moreover, from comparison of the intensity of the 1641.0-keV transition in the total projection spectrum of our data to the 853.64 keV, $2^+ \rightarrow 0^+$ transition of ^{192}Pb [19], which is the strongest transition in our data, we can estimate that the intensity of the ^{97}Nb fragment is ~5% of the intensity of ^{192}Pb, which is the strongest evaporation channel in Experiment I. As a result, the ^{96,97}Nb-gated spectra obtained in Experiment I have better statistics than those from the ^{199}Tl(CN) experiment and, hence, all spectra shown in this work were taken from Experiment I. An example of identification of the 1641.0-keV transition of ^{97}Nb and the 1526.9-keV transition of ^{96}Nb in spectra gated on transitions from complementary fragments is shown in Fig. 5. In the gate of ^{94}Nb in Fig. 5 the 1526.9-keV transition is weak whereas it is stronger in the ^{95}Nb and ^{96}Nb gates. The opposite is true in Fig. 5 for the 1641.0-keV

TABLE I. Transition intensities, corrected for relative efficiency, and their ratios in Sn-gated spectra from Experiment I for selected transitions of $^{94-97}$Nb isotopes.

Isotope	γ ray (keV)	Intensity		Intensity ratio (^{118}Sn/^{117}Sn)
		^{117}Sn-gate	^{118}Sn-gate	
^{97}Nb	1641.0	464(50)	752(50)	1.62(20)
^{96}Nb	194.7	886(80)	1806(90)	2.04(21)
^{95}Nb	824.7	1054(80)	2445(150)	2.32(22)
^{94}Nb	912.6	169(50)	527(80)	3.1(10)

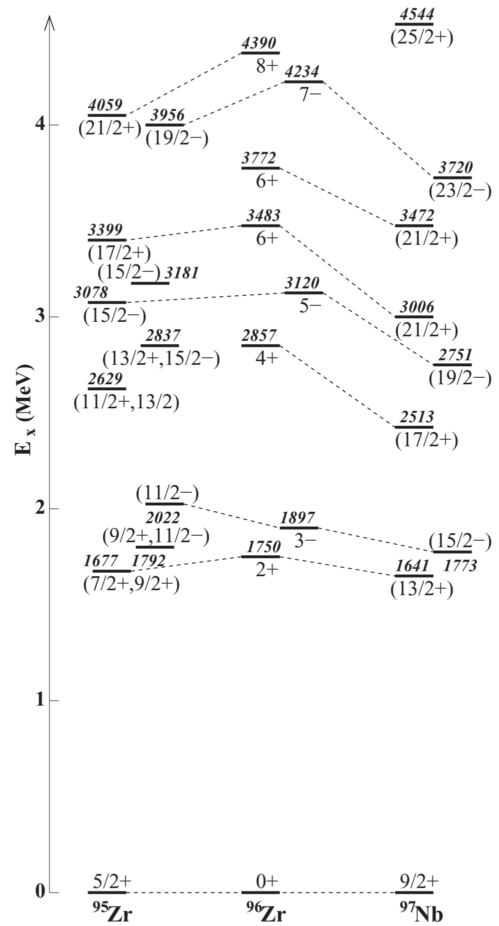

FIG. 8. Comparison of the high-spin states assigned to ^{97}Nb in the present work with known high-spin states in ^{95,96}Zr [8,9].

transition which is strong in the ^{94}Nb and ^{95}Nb gates and disappears in the ^{96}Nb gate, suggesting that the 1641.0-keV transition belongs to an Nb isotope heavier than that of the 1526.9-keV transition. ^{94,95,96}Nb are the $4n$, $5n$, and $6n$ channels with respect to ^{97}Nb and the $5n$, $6n$, and $7n$ channels with respect to ^{96}Nb. For both ^{96}Nb and ^{97}Nb the coincidence in Fig. 5 is stronger in the $5n$ and $6n$ channels whereas it is weaker in the $4n$ channel (weak 1526.9-keV transition in the ^{94}Nb gate) and in the $7n$ channel (1641.0-keV transition not present in the ^{96}Nb gate).

In both experiments the targets included a gold backing and reactions of the beam with the backing produced the ^{221}Pa and ^{220}Th compound nuclei in Experiments I and II, respectively. Hence, the assignment of the transitions in Figs. 1 and 3 to ^{97}Nb and ^{96}Nb, respectively, was further supported by establishing coincidences between these transitions and those from complementary fragments with respect to the ^{221}Pa and ^{220}Th compound nuclei. An example of such coincidences from the ^{197}Pb(CN) experiment is shown in Fig. 6, where gated spectra on transitions assigned to ^{97}Nb and ^{96}Nb are shown. Transitions from the Nb complementary fragments [15–17] with respect to the ^{197}Pb (CN) and the Sn complementary fragments [20–22] with respect to ^{221}Pa(CN) are clearly indicated.

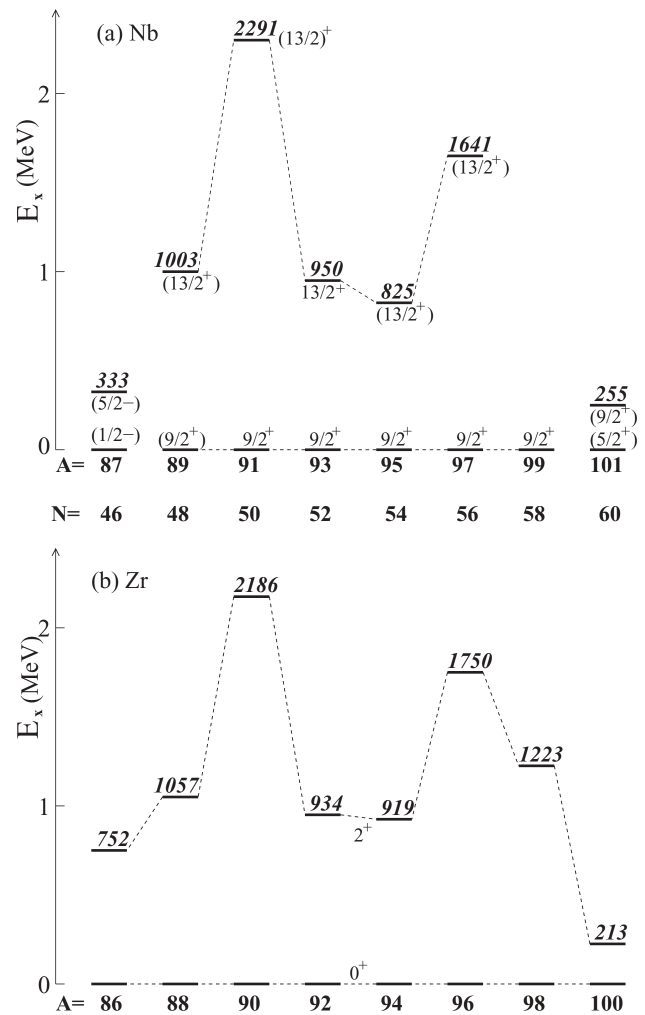

FIG. 9. Systematics for $48 \leqslant N \leqslant 58$ of the first 2^+ excited states in the even-mass Zr isotopes and of the first $13/2^+$ states in the odd-mass Nb isotopes. The ground state $(1/2^-)$ and first $5/2^-$ state of ^{87}Nb, and the ground state $(5/2^+)$ and first $9/2^+$ state of ^{101}Nb are also included. Data from Refs. [9,15,17,24] and the present work.

An additional check of the assignments of the transitions can be deduced from the ratios of γ-ray intensities in complementary-fragment gated spectra. As an example in Fig. 7 the ratios of γ-ray intensities, observed in ^{117,118}Sn-gated spectra, for previously known transitions in the ^{94,95}Nb isotopes and the 194.7- and 1641.0-keV transitions assigned to ^{96,97}Nb, respectively, are shown. The values of the intensities after relative efficiency correction used to obtain these ratios are included in Table I. The ratios for all transitions in Fig. 7 gradually diminish with increasing Nb mass, further supporting the isotopic assignments in the present work.

IV. DISCUSSION

There is very limited high-spin-state information for nuclei in the immediate vicinity of the subshell closure nucleus of $^{96}Zr_{56}$, defined by the following eight isotopes: ^{94,95,96}Y,

^{95,97}Zr, and ^{96,97,98}Nb. High-spin states are known only in ^{95}Zr [8,9] and in ^{95}Y [10]. By establishing high-spin states in two more of these isotopes in the present work, the high-spin-state information around ^{96}Zr is significantly enhanced.

A comparison of the high-spin states established here in ^{97}Nb with those known in ^{95,96}Zr [8,9] is shown in Fig. 8. The first and second excited states, at 1641 and 1173 keV, respectively, are close in energy to the 2^+ and 3^- states in the ^{96}Zr core. This suggests $(13/2^+)$ and $(15/2^-)$ spins and parities for these states in ^{97}Nb and weak coupling of the $g_{9/2}$ proton to the quadrupole and octupole excitations in the core. In addition, the energies and γ-ray decay patterns of the higher-lying states in ^{97}Nb suggest that a one-to-one correspondence can be made between the ^{97}Nb and ^{96}Zr excitations, at least up to 3.7-MeV excitation energy. Specifically, the $(29/2^+) \rightarrow (25/2^+) \rightarrow (21/2^+) \rightarrow (17/2^+) \rightarrow (13/2^+)$ sequence in Fig. 1 is similar to the $(10^+) \rightarrow 8^+ \rightarrow 6^+ \rightarrow 4^+ \rightarrow 2^+$ sequence in ^{96}Zr (see level scheme in Fig. 8 of Ref. [9]) and the $(23/2^-) \rightarrow (19/2^-) \rightarrow (15/2^-)$ sequence in Fig. 1 is similar to the $7^- \rightarrow 5^- \rightarrow 3^-$ sequence in ^{96}Zr. This allows tentative spin-parity assignments for all ^{97}Nb states up to 3.7 MeV, as well as for the 4544- and 5725-keV states in Fig. 1. However, as it can be seen in Fig. 8, the trend of attractive coupling between the odd proton and the excited states of the core is broken for the $(25/2^+)$ state. The same is true for the $(29/2^+)$ state, hence, a similar coupling is not obvious for the higher-lying states just by simply comparing the states in the corresponding level schemes. In ^{95}Zr additional levels have been observed, as shown in Fig. 8, and the interpretation is more complicated, thus, suggesting a less stronger coupling of the $d_{5/2}$ odd neutron hole in ^{95}Zr to the ^{96}Zr core than the $g_{9/2}$ proton coupling to the same core in ^{97}Nb.

The systematics of the first 2^+ excited states in the even-mass Zr isotopes is compared with the systematics of the first $13/2^+$ states in the odd-mass Nb isotopes with number of neutrons between $N = 48$ and $N = 58$ in Fig. 9. The underlying structure changes below $N = 48$ and above $N = 58$, where ^{100}Zr and ^{101}Nb are deformed and $9/2^+$ is no longer the ground state in the odd-mass Nb isotopes. The subshell closures at $N = 50$ in ^{90}Zr and at $N = 56$ in ^{96}Zr result in peaking of the excitation energy of the 2^+ states in these two nuclei in Fig. 9(b). The same behavior is observed in Fig. 9(a) for the odd-mass Nb isotopes with a $9/2^+$ ground state and up to ^{97}Nb. No candidate for a $13/2^+$ state was observed in ^{99}Nb [23], but based on the systematics for the Zr isotopes one could expect such a state at ~1.2-MeV excitation energy.

The addition of a neutron hole in ^{96}Nb to the odd proton of ^{97}Nb results in a much more fragmented level scheme in Fig. 3 compared to the one in Fig. 1. This is expected because there is a larger number of configurations available for excitations from the extra coupling of the neutron hole in ^{96}Nb. The large number of available excitations in this nucleus together with the limited spectroscopic information in neighboring odd-odd nuclei inhibits a fruitful comparison with level schemes in neighboring Nb and Zr isotopes.

High-spin states are known in all the other $N = 56$ isotones in this mass region ($A \leqslant 100$). Specifically, ^{92}Kr and ^{94}Sr were studied as fission fragments in the spontaneous fission of ^{248}Cm [25,26] (no high-spin-state experimental information is known for the neutron-rich $N = 56$ isotones lighter than ^{92}Kr). ^{93}Rb was studied as a fission fragment in the spontaneous fission of ^{252}Cf [27]. ^{95}Y was studied as a fission fragment in the spontaneous fission of ^{248}Cm and ^{252}Cf, as well as in the neutron-induced fission of ^{235}U [10]. ^{96}Zr [28] and ^{98}Mo [29,30], which are stable, have been studied in a variety of methods including Coulomb excitation and the fission fragment method following heavy-ion-induced fusion-evaporation reactions. Finally, the neutron-deficient ^{99}Tc [31] and ^{100}Ru [32] have been studied in a variety of methods including fusion-evaporation reactions. The $9/2^+$ states form the ground state in ^{97}Nb and ^{99}Tc whereas they are isomers in ^{93}Rb and ^{95}Y. The level schemes of high-spin states above the $9/2^+$ states in ^{93}Rb, ^{95}Y, ^{97}Nb, and ^{99}Tc can be compared to the level schemes of the corresponding cores, ^{92}Kr, ^{94}Sr, ^{96}Zr, and ^{98}Mo, respectively. From such a comparison it could be suggested that the level schemes in the ^{97}Nb-^{96}Zr case exhibit the most extensive similarities among these cases. In the case of ^{93}Rb-^{92}Kr, a similar weak-coupling picture of the $g_{9/2}$ proton to the ground band of ^{92}Kr is suggested [27], but the experimental information in ^{93}Rb is limited and similarities can be established for only the first three excited states above the $9/2^+$ isomer. The observation of high-spin states in ^{97}Nb in the present work completes the picture of the systematics of the $N = 56$ isotones in this mass region.

The results of the shell-model calculations in Ref. [4] predict the first $13/2^+$ state in ^{97}Nb at ~1.5-MeV excitation energy. The tentative spin-parity assignment of $13/2^+$ to the 1641-keV state observed in ^{97}Nb in the present work is in very good agreement with this prediction, although in the same calculation, the first 7^+ state in ^{96}Nb is predicted at ~0.5-MeV excitation energy, whereas experimentally it is observed at a much lower excitation energy. Clearly, new shell-model calculations for high-spin states in ^{96,97}Nb are needed for a wider comparison with the experimental results presented in this work.

V. SUMMARY

In summary, high-spin states were observed for the first time in ^{96,97}Nb following the fission of hot compound nuclei formed in two different fusion-evaporation reactions. The assignment of the transitions is based on coincidences with previously known transitions in the complementary fragments. Excited states in ^{97}Nb up to 3.7 MeV can be interpreted as the coupling of the odd proton occupying the $g_{9/2}$ orbital to positive and negative parity yrast states in the ^{96}Zr core. A comparison with the first excited states in ^{95}Zr suggests a weaker coupling of the $d_{5/2}$ odd neutron hole in ^{95}Zr to the ^{96}Zr core. A much more fragmented level scheme is observed in ^{96}Nb from the coupling of both the odd proton particle and the odd neutron hole to the states in the ^{96}Zr core. The spectroscopy of high-spin states in the immediate vicinity of the subshell closure nucleus ^{96}Zr is now more complete and the gap at $A = 97$ in the systematics of high-spin states in $N = 56$ isotones is now bridged. More experimental information, especially firm spin and parity assignments of the high-spin states reported here, is needed to confirm the interpretations suggested in the present work. The extensive level schemes for ^{96,97}Nb now available show the need for new shell-model calculations for nuclei near ^{96}Zr.

ACKNOWLEDGMENTS

This work was supported in part by the US Department of Energy under Contract Nos. DE-AC52-06NA25396 (LANL), DE-AC52-07NA27344 (LLNL), and AC03-76SF00098 (LBNL), and by the National Science Foundation (Rutgers).

[1] N. Nica, Nucl. Data Sheets **111**, 525 (2010).
[2] K. Krishan and S. Sen, Phys. Rev. C **18**, 1026 (1978).
[3] P. K. Bindal, D. H. Youngblood, R. L. Kozub, and P. H. Hoffmann-Pinther, Phys. Rev. C **12**, 390 (1975).
[4] D. H. Gloeckner, Nucl. Phys. A **253**, 301 (1975).
[5] K. Takahashi, G. J. Mathews, and S. D. Bloom, Phys. Rev. C **33**, 296 (1986).
[6] D. Abriola and A. A. Sonzogni, Nucl. Data Sheets **109**, 2501 (2008).
[7] K. Zajac, Int. J. Mod. Phys. E **13**, 103 (2004).
[8] N. Fotiades *et al.*, Phys. Rev. C **65**, 044303 (2002).
[9] D. Pantelica *et al.*, Phys. Rev. C **72**, 024304 (2005).
[10] W. Urban *et al.*, Phys. Rev. C **79**, 044304 (2009).
[11] N. Fotiadis, in *Proceedings of the Fourth International Conference on Fission and Properties of Neutron-Rich Nuclei, Sanibel Island, USA, November 11–17, 2007*, edited by J. H. Hamilton, A. V. Ramaya, and H. K. Carter (World Scientific Publishing, Singapore, 2008), p. 542.
[12] N. Fotiades *et al.*, Phys. Rev. C **71**, 064312 (2005).
[13] N. Fotiades *et al.*, Phys. Rev. C **67**, 034602 (2003).
[14] R. Krücken *et al.*, Eur. Phys. J. A **5**, 367 (1999).
[15] C. M. Baglin, Nucl. Data Sheets **80**, 1 (1997).
[16] D. Abriola and A. A. Sonzogni, Nucl. Data Sheets **107**, 2423 (2006).
[17] D. Bucurescu *et al.*, Phys. Rev. C **71**, 034315 (2005).
[18] N. Fotiades *et al.*, Phys. Scr., T **88**, 127 (2000).
[19] C. M. Baglin, Nucl. Data Sheets **84**, 717 (1998).
[20] J. Blachot, Nucl. Data Sheets **95**, 679 (2002).
[21] K. Kitao, Nucl. Data Sheets **75**, 99 (1995).
[22] D. M. Symochko, E. Browne, and J. K. Tuli, Nucl. Data Sheets **110**, 2945 (2009).
[23] L. K. Peker, Nucl. Data Sheets **73**, 1 (1994).
[24] R. B. Firestone, V. S. Shirley, C. M. Baglin, S. Y. Frank Chu, and J. Zipkin, *Table of Isotopes* (Wiley, New York, 1996), and references therein.
[25] T. Rząca-Urban *et al.*, Eur. Phys. J. A **9**, 165 (2000).
[26] T. Rząca-Urban, K. Sieja, W. Urban, F. Nowacki, J. L. Durell, A. G. Smith, and I. Ahmad, Phys. Rev. C **79**, 024319 (2009).
[27] J. K. Hwang *et al.*, Phys. Rev. C **80**, 037304 (2009).
[28] A. A. Sonzogni, Nucl. Data Sheets **109**, 2501 (2008).
[29] B. Singh and Z. Hu, Nucl. Data Sheets **98**, 335 (2003).
[30] S. Lalkovski *et al.*, Phys. Rev. C **75**, 014314 (2007).
[31] J. K. Tuli, G. Reed, and B. Singh, Nucl. Data Sheets **93**, 1 (2001).
[32] B. Singh, Nucl. Data Sheets **109**, 297 (2008).